IMPEDIMENTRIC AND MICROSCOPIC PROBES OF THE INTEGRITIES OF SELF-ASSEMBLED MONOLAYERS OF ORGANOSULPHUR-METAL COMPLEXES

Akinbulu, I. A.*[1]; Ogunbayo, B. T.[1]; Modibane, K.D.[2] and Gcineka, M.[3]

[1]Department of Chemistry, University of Lagos, Lagos, Nigeria

[2]Department of Chemistry, University of Limpopo, Sovenga, South Africa

[3]Department of Chemistry, University of the Western Cape, Cape Town, South Africa

*(Corresponding Author: iakinbulu@unilag.edu.ng; Tel. No. +2348133785236)

(Received: 29th Feb., 2016; Accepted: 27th April, 2016)

ABSTRACT

Electrical and structural integrities of Self-assembled Monolayers (SAMs) of some organosulphur-metal complexes, formed on polycrystalline gold disc electrode, were probed, using Electrochemical Impedance Spectroscopy (EIS) and Atomic Force Microscopy (AFM) respectively. Values of relevant circuit elements in the equivalent circuits, proposed to explain the physical electrochemistry of the cells, were a reflection of the electrical conductivity of the SAM-modified gold electrodes. Electrical integrity of SAMs was influenced by both the metal center and molecular identity of the substituent, attached to the ligand framework, in the chemical modifier of interest. AFM images of the SAMs were indicative of their structural integrity. SAM formed from organosulphur-metal complex containing diethylaminoethanethio substituent (**4**-SAM) was more compact than those formed from organosulphur-metal complexes containing benzylthio substituent (**1**-**3**-SAMs). This was typical of SAMs formed from alkanethio and alkylthio substituted metallophthalocyanine complexes.

Keywords: Electrochemical Impedance Spectroscopy, Atomic Force Microscopy, Self-assembled Monolayer, Organosulphur-metal Complex, Metallophthalocyanine

INTRODUCTION

Self-assembled Monolayer (SAM) is a single molecular layer in which the constituents share similar orientation. SAM is formed by the adsorption of molecules onto a suitable substrate from a homogeneous solution. This monolayer is highly organized and stable, due to the affinity of the head group for the substrate and possible interactions between closely packed tail groups. Self-assembly is one of the numerous techniques employed in the fabrication of Chemically Modified Electrodes (CMEs). This technique is not new, but its popularity can be traced to the series of works published by Sagiv (Polymeropoulos and Sagiv, 1978; Sagiv, 1979; Sagiv, 1980) on highly stable SAMs of alkanesilanes formed on glass and aluminium oxide substrates. The growth of this technique was given further impetus by the discovery of Allara and Nuzzo (Nuzzo and Allara, 1983; Allara and Nuzzo, 1987). Their ingenious act of forming SAMs of organosulphur derivatives (thiols), disulfides, sulfides, and related moieties, on metal substrates (such as Au, Pt and Hg) was a watershed in the broader field of chemically modified electrodes. The organization and stability of this class of SAMs can be attributed to the strong interaction between sulphur and these substrates, particularly gold. The interaction between sulphur and gold is strong, specific and selective. The strength of Au-S bond is reported to be in the order of 40-50 kcal/mol (Nuzzo *et al*, 1987).

The organosulphur-metal complexes of interest in this work are thio-derivatized metallophthalocyanine complexes, while the substrate of choice is gold. The interest in metallophthalocyanine complexes is informed by their extensive applications. Self-assembled monolayers of thio-derivatized metallophthalocyanine complexes are frequently employed as electrocatalysts and in the fabrication of electrochemical sensors (Ozoemena *et al.*, 2003; Simpson *et al.*, 1995). Other uses of the SAMs of these macrocycles include: corrosion prevention (Chen *et al.*, 1999) and design of molecular electronic devices (Finklea, 2000).

The uses of SAMs of thio-derivatized metallophthalocyanine complexes for design of electrochemical sensors and molecular electronic devices can be closely associated with the electrical conductivity and structural features of these SAMs. These important properties can be fully

maximized and better understood by designing methods that can probe the electrical and structural integrities of these SAMs. A simple, but reliable, technique of probing the electrical integrity of SAMs of these interesting organosulphur-metal complexes is electrochemical impedance spectroscopy, EIS, while their structural integrity will be investigated, using atomic force microscope. Atomic force microscopy is a very useful and invaluable technique in probing the structural integrity of surfaces, which is important in investigating the suitability of SAM in corrosion prevention. Other methods that are routinely employed in probing the structural integrity of SAMs of organosulphur derivatives include: measurement of wetting contact angle, infra red and Raman spectroscopy, ellipsometry, x-ray photoelectron spectroscopy (XPS) (a high vacuum surface method) and microscopy (scanning tunneling and scanning electron microscopies).

Impedance (Z) is a complex quantity associated with an alternating current (ac) circuit, analogous to resistance (R) in a direct current (dc) circuit. It is a vector quantity, thus has magnitude ($Z_o = V_o/I_o$) and phase (Φ), where V_o and I_o are the voltage and current amplitudes respectively. As a result, Z has both imaginary and real components, represented by equation 1.

$$Z = Z_o(\cos\Phi + j\sin\Phi) = Z' + jZ'' \quad (1)$$

where $j = \sqrt{(-1)}$, while Z' and Z'' are the real and imaginary components of the impedance. The complex plane showing these components is depicted in Figure 1.

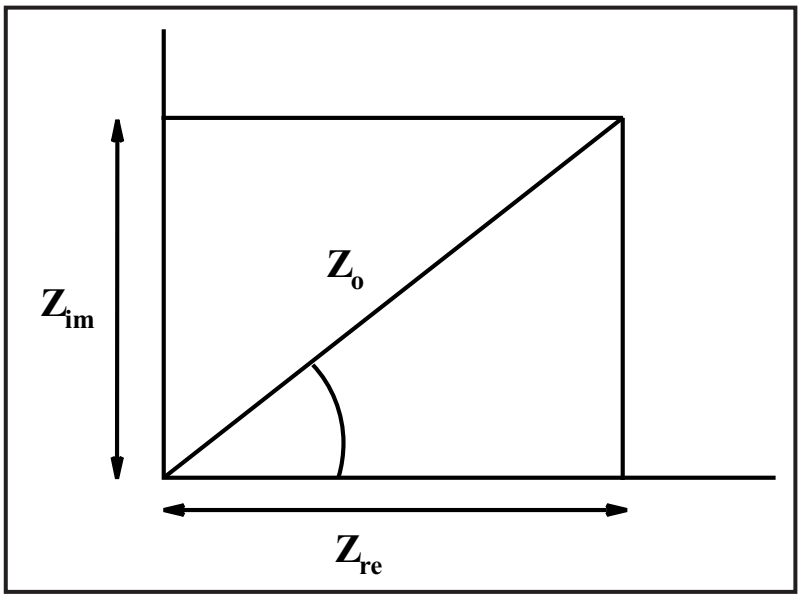

Figure 1: Complex plane showing real and imaginary components of impedance

In EIS, an electrical stimulus, in the form of a specified voltage (the former potential of the redox probe of interest), is applied to the working electrode, resulting in the polarization of the electrode/solution interface. Impedance of the cell is then sampled over a specified range of frequencies, resulting in a plot of imaginary versus real impedance, Nyquist plot (Barsoukov and Macdonald, 2005). Application of this technique to electrochemical phenomena relies on the use of different circuit models (the equivalent circuits), depending on the impedance spectrum in the complex plane, to explain the physical electrochemistry of the cell. Apart from the use of networks of electrical circuit elements, EIS data can also be analyzed using a mathematical model that predicts the theoretical impedance of the cell. The former is used in this work.

The use of equivalent circuit to explain the physical electrochemistry of a three-electrode electrochemical cell takes into account three

important parameters in the cell (Barsoukov and Macdonald, 2005). The first parameter is the resistance of the electrolyte solution between the reference and the working electrodes (R_S). A resistor, with resistance (impedance) equal to R_S accounts for this parameter in the equivalent circuit. Another relevant parameter is the double-layer capacitance (C_{dl}) of the electrochemical double layer, a capacitor-like interfacial region in the cell. This parameter is taken into consideration by the inclusion of a capacitor, with capacitance equal to C_{dl}, in the equivalent circuit. The third parameter is the resistance (impedance) of the charge-transfer process (R_{CT}). In the equivalent circuit, this is represented by a resistor, with resistance equal to R_{CT}. The equivalent circuit comprising of these parameters is a parallel combination of R_{CT} and C_{dl}, in series with R_S. This circuit can be modified to account for other physical processes in the cell, depending on the impedance spectrum of interest. One of such modification is the inclusion of the Warburg impedance, Z_W, to account for diffusion-related process in the cell.

The structures of the thio-derivatized metallophthalocyanine complexes used in this work are shown in Figure 2. These complexes are designated **1-4**. As shown in Figure 2, complexes **1**, **2** and **3** are cobalt, manganese and iron complexes respectively; having the same substituent (benzylthio), attached to the phthalocyanine ligand skeleton, while complex **4** is an iron complex, with a different substituent (diethylaminoethanethio). The inclusion of complex **4** is aimed at investigating the integrities of SAMs of organosulphur-metal complexes of the same metal (complexes **3** and **4**) but with different molecular architecture. The synthesis of complex **4** has been reported (Akinbulu *et al.*, 2010). Also complexes **1**, **2** and **3** have been synthesized and characterized (Akinbulu *et al.*, 2011). The formation and electrochemical characterization of SAMs of these complexes have also been reported (Akinbulu *et al.*, 2010; Akinbulu *et al.*, 2011).

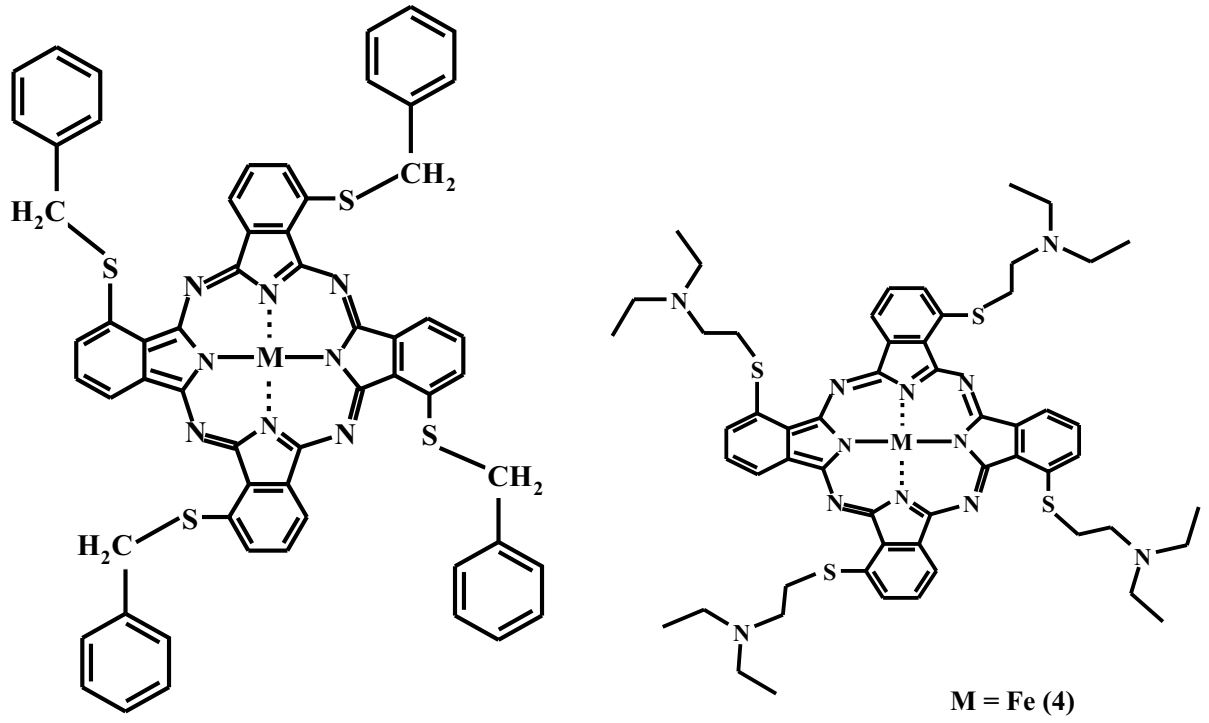

Figure 2: Molecular structures of metallophthalocyanine complexes

METHODOLOGY

Electrochemical Studies

Electrochemical experiments were performed using Autolab potentiostat PGSTAT 302 (Eco Chemie, Utrecht, The Netherlands) driven by the general purpose Electrochemical System data processing software (GPES, software version 4.9). A conventional three-electrode system was used. The working electrode was polycrystalline gold disc electrode, modified with the SAM of the thio-derivatized metallophthalocyanine complex of interest. The SAM-modified gold disc electrodes are designated **1**-SAM, **2**-SAM, **3**-SAM and **4**-SAM.Ag | AgCl (3M KCl) and platinum wire were used as reference and auxiliary electrodes respectively. Electrochemical impedance spectroscopy measurements were performed with Autolab FRA software between 1.0 mHz and 10 KHz using a 5 mV rms sinusoidal modulation, in 1 mM solution of $K_3Fe(CN)_6$ (redox probe) containing 0.1 M KCl as supporting electrolyte, at half-wave potential of the $[Fe(CN)_6]^{3-}/[Fe(CN)_6]^{4-}$ redox couple (0.10 V versus Ag | AgCl (3M KCl)). A non-linear least squares (NNLS) method based on the EQUIVCRT programme (Boukamp, 1986) was used for automatic fitting of the obtained EIS data.

Microscopic Study

Atomic force microscope was used, in the non-contact mode in air, to probe the structural integrity of the SAMs. Microscopic study was carried out with SAMs formed on gold-coated glass. The SAMs were formed by immersing the gold-coated glass in the solution of the organosulphur-metal complex of interest, for 24 hours.

RESULTS AND DISCUSSION

Cyclic Voltammetry Responses of SAM-modified Gold Electrodes in $K_3Fe(CN)_6$

The cyclic voltammetry responses of the SAM-modified gold electrodes in 1 Mm solution of $K_3Fe(CN)_6$, containing 0.1 M KCl supporting electrolyte (Figure 3), were investigated. This was necessitated by the need to seek for a preliminary understanding of the dynamics of electron transport within the SAMs, thus providing a conservative measure of their electrical integrity.

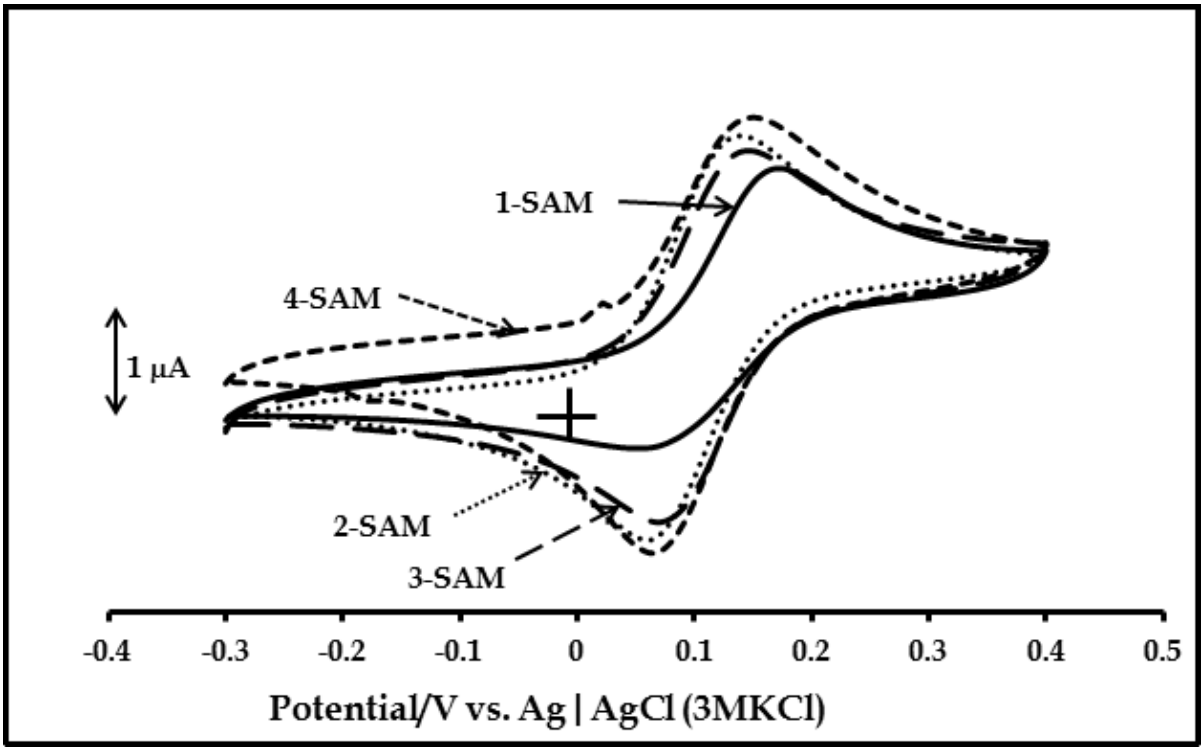

Figure 3: Cyclic voltammetry profiles of SAM-modified gold electrode in 1 mM solution of $K_3Fe(CN)_6$, containing 0.1 M KCl supporting electrolyte. Scan rate: 25 mVs^{-1} versus Ag | AgCl

$K_3Fe(CN)_6$ was used as redox probe because of the characteristic reversible nature of the$[Fe(CN)_6]^{3-}/[Fe(CN)_6]^{4-}$ redox process. As a result, the value of peak splitting, ΔE, for this process, on each of the SAM-modified gold electrodes, could be a conservative estimate of the rate of electron transport within the cell of interest.

The values of ΔE for the cells with the different SAM-modified gold electrodes are indicated in Table 1. They are 117, 73, 67 and 80 mV versus Ag|AgCl (3M KCl) for **1**-SAM, **2**-SAM, **3**-SAM and **4**-SAM-modified gold electrodes respectively. These values suggest that electron transport is fastest in the cell with**3**-SAM-modified gold electrode and slowest in the cell with **1**-SAM-modified gold electrode. This observation establishes the likelihood of the dependence of electrical integrity of SAM on the chemistry of the metal center and molecular nature of substituent, attached to the ligand, in the organosulphur-metal complex.

Table 1: Peak separation and EIS data for the cells with the SAM-modified gold electrodes

SAM-modified electrode	ΔE (mV)	R_S (KΩ)	R_{CT} (KΩ)	C_{dl} (μF)	Z_W ($\Omega\ S^{-1/2}$) $\times 10^{-5}$	ω (Hz)	Phase Angle (°)	*n*
1-SAM	117	0.71 ± 0.03	18.80 ± 0.70	0.13 ± 0.01	3.77 ± 0.30	398	61	0.85
2-SAM	73	0.51 ± 0.01	1.66 ± 0.10	0.32 ± 0.01	4.75 ± 0.10	501	36	0.78
3-SAM	67	0.38 ± 0.01	0.71 ± 0.02	0.43 ± 0.01	5.49 ± 0.10	501	32	0.81
4-SAM	80	0.69 ± 0.01	6.08 ±0.21	0.01 ±0.001	-	16	49	0.68

It should be recalled that**3**-SAM- and **4**-SAM-modified gold electrodes were constructed from iron complexes (Akinbulu *et al.*, 2011; Akinbulu *et al.*, 2010), while the modifiers in**1**-SAM and **2**-SAM-modified gold electrodes contain cobalt and manganese metal centers respectively (Akinbulu *et al.*, 2011) (Figure 2). The relatively enhanced electron transport within the cellwith**3**-SAM-modified gold electrode, compared to the cells with **1**-SAM and **2**-SAM-modified gold electrodes, attests to the effect of metal center on electrical nature of the SAMs. This observation may be interpreted in terms of the readiness or ease with which loss of electron, accompanying the change from d^6 configuration to a much more stable d^5 configuration, occurs in iron complexes. This change is associated with Fe^{3+}/Fe^{2+} redox process, whose occurrence has been reported, not only for the solution electrochemistry of complex **3** and **4**, but also for their adsorbed species (Akinbulu *et al.*, 2011; Akinbulu *et al.*, 2010).

Comparison of the results obtained for **3**-SAM- and **4**-SAM-modified gold electrodes illustrates the effect of molecular identities of substituents, attached to the phthalocyanine ligand framework, in the metal complexes, on electron transport within the cells having these electrodes. The substituents are benzylthio and diethylaminoethanethio, as highlighted previously, for **3**-SAM and **4**-SAM-modified gold electrodes respectively (Figure 2). The relatively better electron transport within the cell with**3**-SAM-modified gold electrode (ΔE = 67 mV), compared to the cell with**4**-SAM-modified gold (ΔE = 80 mV), may be explained in terms of the relatively enriched electron density of **3**-SAM, attributable to the delocalized π-electrons of the benzyl substituent of the chemical modifier employed in fabricating the electrode. The same reason (effect of substituent) can be offered for the lower value of ΔE, for **2**-SAM (benzylthio substituent), compared with that for **4**-SAM (diethylaminoethanethio substituent).

Impedance Spectra of SAM-modified Gold Electrodes in $K_3Fe(CN)_6$

Figures 4 and 5 are the impedance spectra (Nyquist plots) of the SAM-modified gold electrodes in 1 mM solution of $K_3Fe(CN)_6$, containing 0.1 M KCl supporting electrolyte. The impedance spectra of **1**-SAM, **2**-SAM and **3**-SAM-modified gold electrodes (Figure 4) depict semi-circles, characteristic of charge transfer-dependent impedance, in the high- frequency region, and straight lines, which are signatures of purely diffusion-mediated reactions, in the low-frequency domain.

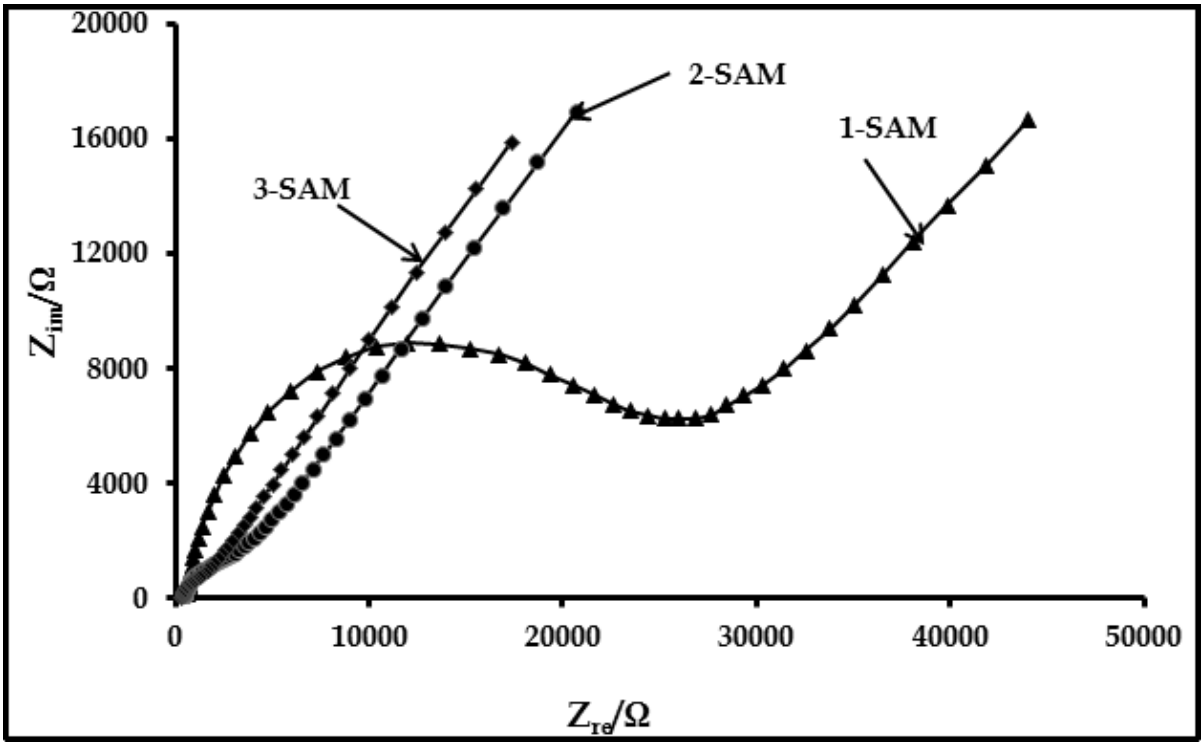

Figure 4: Nyquist plots of the SAM-modified gold electrodes (**1**-SAM, **2**-SAM and **3**-SAM) in 1 mM solution of $K_3Fe(CN)_6$, containing 0.1 M KCl supporting electrolyte. Applied potential = 0.10 V versus Ag | AgCl (3KCl)

The impedance spectrum of **4**-SAM-modified gold electrode is shaped like an arc (Figure 5). The spectrum is devoid of a well-resolved semi-circular region and the distinct straight line, characteristic of the impedance spectra of the other SAM-modified gold electrodes (Figure 4). This spectrum thus has a minimal feature of charge transfer-limited behaviour and a negligible diffusion-controlled nature.

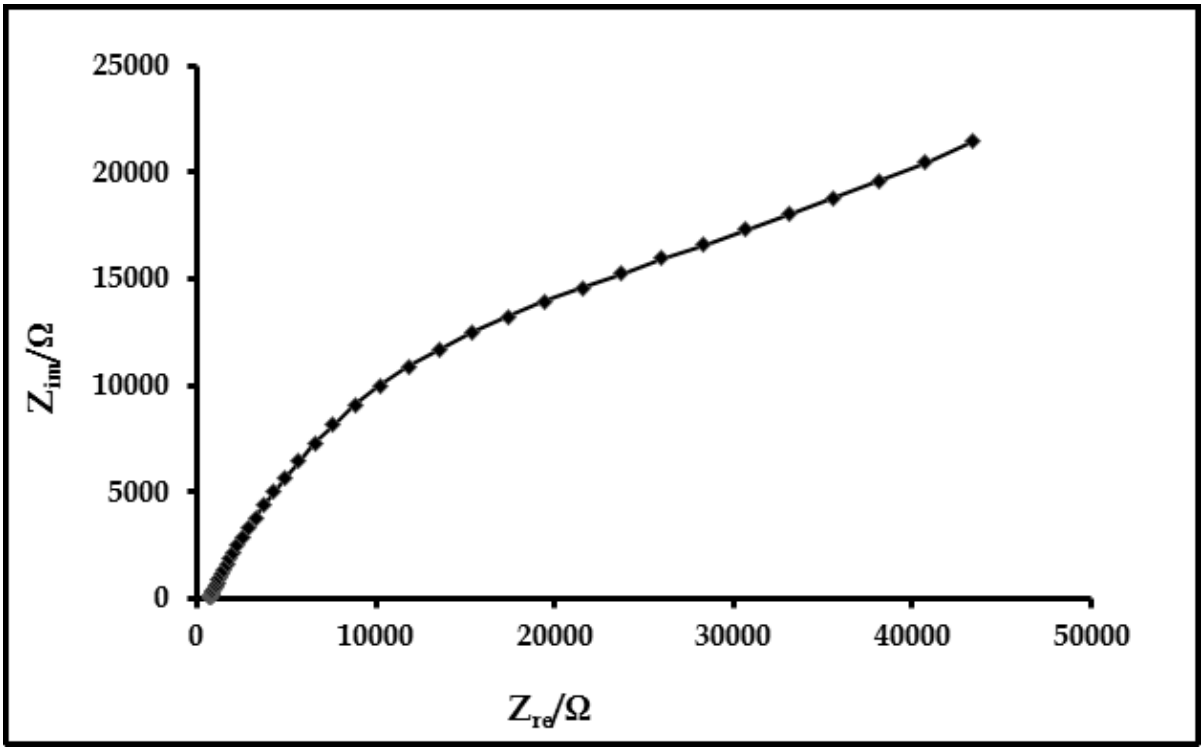

Figure 5: Nyquist plots of the **4**-SAM-modified gold electrode in 1 mM solution of $K_3Fe(CN)_6$, containing 0.1 M KCl supporting electrolyte. Applied potential = 0.10 V versus Ag | AgCl (3KCl)

Equivalent Circuits and Fitting of Impedance Data

The equivalent circuit that is consistent with the impedimentary attributes displayed in Figure 4 is shown in Figure 6A, where R_S is the resistance of the electrolyte solution between the reference and the working electrodes, R_{CT} is the charge transfer resistance, Z_W is mass-transfer or Warburg impedance and C_{dl} is the double-layer capacitance, that models the capacitance of the electrochemical double layer of the cell. The magnitudes of these components and their percentage errors are shown in Table 1. These values are direct measures of the electrical integrity of these SAMs, discussed later in this work.

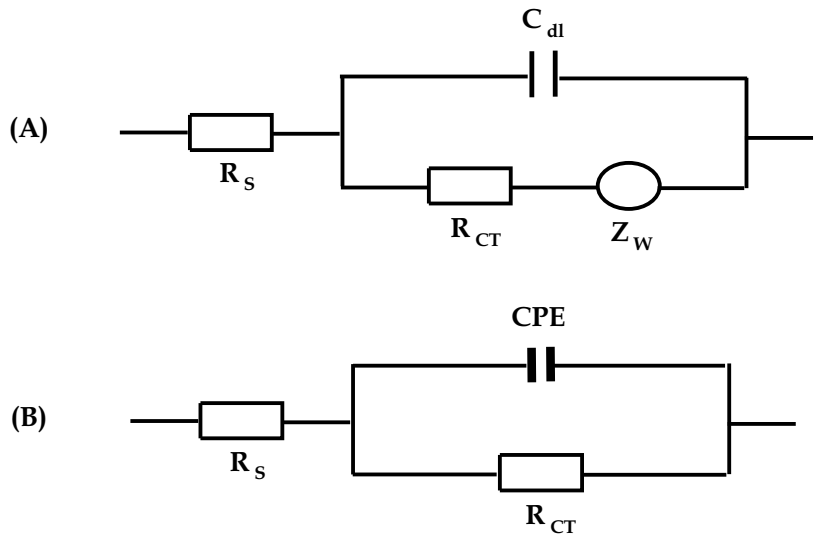

Figure 6: (A) Proposed equivalent circuits for the impedance spectral of the cells with (**1**-**3**)-SAM-modified gold electrodes, (B) equivalent circuit for the cell with **4**-SAM- modified goldelectrode.

As shown in Table 1, values of R_S, **1**-SAM (0.71 K**Ω**), **2**-SAM (0.51 K**Ω**) and **3**-SAM (0.38 K**Ω**), are closely related. This is not unexpected, since the magnitude of R_S is a function of the nature and concentration of the electrolyte. Nonetheless, it is interesting to know that these values are consistent with the values of ΔE for the SAMs, Table 1. The cell with the most impressive rate of electron transport (the cell with **3**-SAM-modified gold electrode) has the lowest value of R_S.

In-depth evaluation of the magnitudes of other circuit components (R_{CT}, C_{dl} and Z_W) establishes a close relationship between electrical integrity and the nature of the metals in the complexes constituting the SAMs. It suggests that the conducting backbones of SAMs are closely linked to the metal centers in the organosulphur-metal complexes, the building blocks of the SAMs. The relatively enhanced electrical conductivity of the cell with **3**-SAM-modified gold electrode, as shown by the impressive value of R_{CT} (0.71 K**Ω**), compared to those with **1**-SAM (18.80 K**Ω**) and **2**-SAM-modified gold electrodes (1.66 K**Ω**) (Table 1), may be interpreted in terms of the electronic stability and the ease of electron loss, associated with the change from d^6 (Fe^{2+}) to d^5 (Fe^{3+}) configuration. It should be recalled that **3**-SAM-modified gold electrode was fabricated from an iron complex (Akinbulu *et al.*, 2011) (Figure 2). This change is the driver of Fe^{3+}/Fe^{2+} redox process, which occurs readily within **3**-SAM, as previously highlighted. This may have promoted charge transfer phenomenon within the cell, resulting in good electrical conductivity. There is also some measure of consistency between values of R_{CT} and ΔE for the cells (Table 1). The cell with the lowest ΔE equally has the lowest R_{CT}, thus suggesting that enhanced electron transport within the cell with **3**-SAM-modified gold electrode is the direct consequence of the lowest value of charge transfer resistance, R_{CT}, associated with the cell.

Evaluation of values of C_{dl} for the cells with the different SAM-modified gold electrodes further unravels the electrical integrity of the SAMs. The value of capacitance, a measure of the capacitive property of the cell, is a conservative estimate of its capacity to store electrical charges. The cell with the highest charge storage capacity is the cell with **3**-SAM-modified gold electrode, with a capacitance, C_{dl}, of 0.43 μF (Table 1). The fact that this cell has the highest rates of electron transport (ΔE = 67 mV) and charge transfer (R_{CT} = 0.71 K**Ω**), coupled with its relatively impressive ability to store electrical charges (C_{dl} = 0.43 μF) (Table 1), make the **3**-SAM-modified gold electrode the best electrically conducting, out of all the surfaces probed.

Analysis of the values of Warburg impedance, Z_W, equally contributes to a better understanding of the electrical integrity of the SAMs. The value of Z_W is closely related to the extent of diffusion of charged species or electrolytes within the cell. The farther the diffusion of charged species, the higher the value of Z_W and vice versa. The fact that rate of charge transfer is highest in the cell with **3**-SAM-modified gold electrode, as discussed previously, suggests that charged species diffused farthest within this cell, thus justifying its highest value of Z_W (5.49×10^{-5} **Ω** $s^{-1/2}$) (Table 1). Generally, values of Z_W for the cells are consistent with the rates of charge transfer or the values of charge transfer resistance, R_{CT}, (Table 1). The cell (**1**-SAM-modified gold electrode) with the highest value of R_{CT} (18.80 K**Ω**) or lowest rate of charge transfer has the lowest value of Z_W (3.77×10^{-5} **Ω** $s^{-1/2}$).

The shape of the impedance spectrum of **4**-SAM-modified gold electrode (Figure 5) is different from those of the other SAM-modified gold electrodes. This difference can be attributed to the difference in molecular identity of substituent, attached to the ligand skeletal frame, in the iron complex, from which the SAM was fabricated (Figure 2). The impedance spectrum is arc-like in shape, as highlighted previously. Hence the use of the equivalent circuit in Figure 6A, which consists of only ideal circuit elements, to analyze the impedance data, resulted in error. The circuit proposed to analyze this impedimentary behavior is shown in Figure 6B. This circuit is made up of solution resistance, R_S, in series with a parallel combination of charge transfer resistance, R_{CT}, and constant phase element, CPE, which replaces the double-layer capacitance, C_{dl}. Expectedly, Warburg impedance, Z_W, is not included as circuit

element, since the impedance spectrum in Figure 5 is associated with negligible diffusion-mediated impedance attribute. CPE is a distributed circuit element, which is an empirical representation of the deviation of double-layer capacitance, C_{dl}, from ideality.

Impedance behavior, explained by substituting CPE for C_{dl}, was reported by Brug and coworkers in 1984 (Brug *et al*, 1984). They observed the anomalous dispersion behavior of capacitance as a sloping line, in the complex plane plot for the impedance of a serial combination of resistor and capacitor, *RC*, unlike the characteristic vertical linear line for the same *RC* circuit. For a Faradaic process involving a reaction-kinetic resistance (charge transfer resistance), in parallel with double layer capacitance element, a depressed semicircle, with its center on the real axis of the complex plane, was reported. The ill-resolved semicircle associated with the impedance spectrum in Figure 5 is analogous to the depressed semicircle reported by Brug *et al.*(1984), justifying the inclusion of charge transfer resistance, R_{CT}, in parallel with CPE, in the proposed circuit in Figure 6B. The true capacitance, C, was estimated from the value of CPE by using equation 2 (Hsu and Manfeld, 2001).

$$C = Q^{o}(\omega_{max})^{n-1} \qquad 2$$

Where *C* is the true capacitance, Q^o is the CPE and ω_{max} is the frequency corresponding to the maximum value of impedance.

The solution resistance, R_S, for the cell with **4**-SAM-modified gold electrode (0.69 K**Ω**) is not substantially different from those of the other cells. The circuit element of interest is the charge transfer resistance, R_{CT}. The value for the cell with **4**-SAM-modified gold electrode (6.08 K**Ω**) is significantly different from that for the cell with **3**-SAM-modified gold electrode (0.71 K**Ω**). This huge difference can be attributed to better electrical conductivity of **3**-SAM-modified gold electrode, resulting from increased electron density of the SAM. Increase in electron density may be attributed to the presence of delocalized π-electrons of the benzyl substituent of the chemical modifier, employed in designing the modified-electrode. The values of R_{CT} for the two cells equally agree with the values of peak splitting, Δ*E* (67 mV for **3**-SAM- and 80 mV for **4**-SAM-modified gold electrode) (Table 1). Lower R_{CT} can be associated with lower Δ*E*, which translates to better charge transfer, faster rate of electron transport and increased electrical conductivity.

Bode Plots of SAM-modified Gold Electrodes in $K_3Fe(CN)_6$

Figure 7 are Bode plots (phase angle versus logarithm of frequency) derived from the Nyquist plots for the SAM-modified gold electrodes. Data derived from Bode plots (Table 1) also offers some measure of understanding of the electrical integrity of the SAMs. Phase angle, Φ, for each of the SAM-modified gold electrodes is less than 90° (Table 1). For ideal capacitor, Φ is 90°. The closer to 90°, the more capacitive, rather than conducting, the nature of the SAM-modified gold electrode is. The values of phase angles are in agreement with the electrical integrities of the SAMs (Table 1). The SAM (**3**-SAM) with the lowest phase angle (32°) is the best conducting of all the SAMs. This is consistent with the values of Δ*E* (67 mV) and R_{CT} (0.71 KΩ) for this SAM.

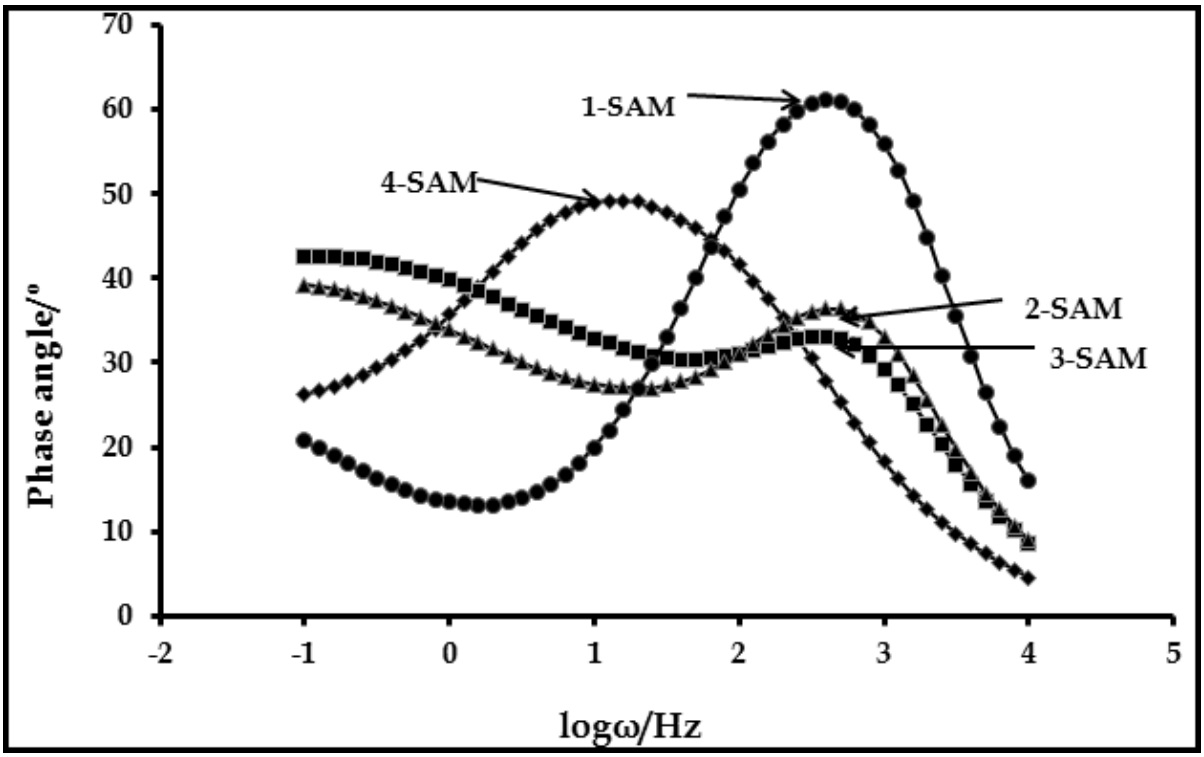

Figure 7: Bode plots (phase angle versus log ω) obtained for the cells with (**1**-**4**)-SAM- modified gold electrodes in 1 mM solution of $K_3Fe(CN)_6$ containing 0.1 M KCl as the supporting electrolyte. Applied potential = 0.10 V versus Ag | AgCl (3KCl)

The least conducting of the SAMs (**1**-SAM) has a phase angle of 61°, the closest to 90°. Also, this agrees with the values of ΔE (117 mV) and R_{CT} (18.8 KΩ) for this SAM.

AFM Images of SAMs

AFM images of bare gold-coated glass and the SAM-modified gold-coated glasses are shown in Figure 8. The bare gold-coated glass (Figure 8A), expectedly, shows a very rough nature. It has a mean roughness of 0.11 nm. The AFM image of **4**-SAM (Figure 8B) shows a more compact and closely packed SAM than that of the porous and less compact **3**-SAM (Figure 8C). **4**-SAM has a thickness (difference in thickness between SAM-modified and bare gold-coated glasses) of 0.015μm, and mean roughness of 0.65 nm. The AFM image of **3**-SAM (Figure 8C) is representative of the AFM images of **1**-**3**-SAMs. The SAM has a thickness of 0.0016 μm, and mean roughness of 0.25 nm. The AFM images of the SAMs are consistent with the values of ion barrier factor, Γ_{ibf}, reported for these SAMs, with values of 0.82, 0.76, 0.79 and 0.87 respectively for **1**-**4**-SAMs (Akinbulu *et al*, 2010; Akinbulu *et al*, 2011). Ion barrier factor is a measure of how closely packed or defect-free a SAM is. The closer to unity the value of Γ_{ibf}, the more closely packed or defect-free the SAM. The obvious difference in structural integrity of **3**-SAM and **4**-SAM can be associated with the molecular nature of the substituent on the ligand skeleton of the modifier of interest. This suggests that, the diethylaminoethanethio (an alkylthio) substituent in **4-**SAM, unlike the benzylthio substituent in **1**-**3**-SAMs, aids the formation of a more closely packed or relatively defect-free SAM. Such a closely packed nature has also been observed in the SAMs of alkanethiols (Porter *et al*., 1987). This implies that, a relatively defect-free **4**-SAM, though not electrically conducting as **3**-SAMs, may be a better candidate for use in corrosion prevention.

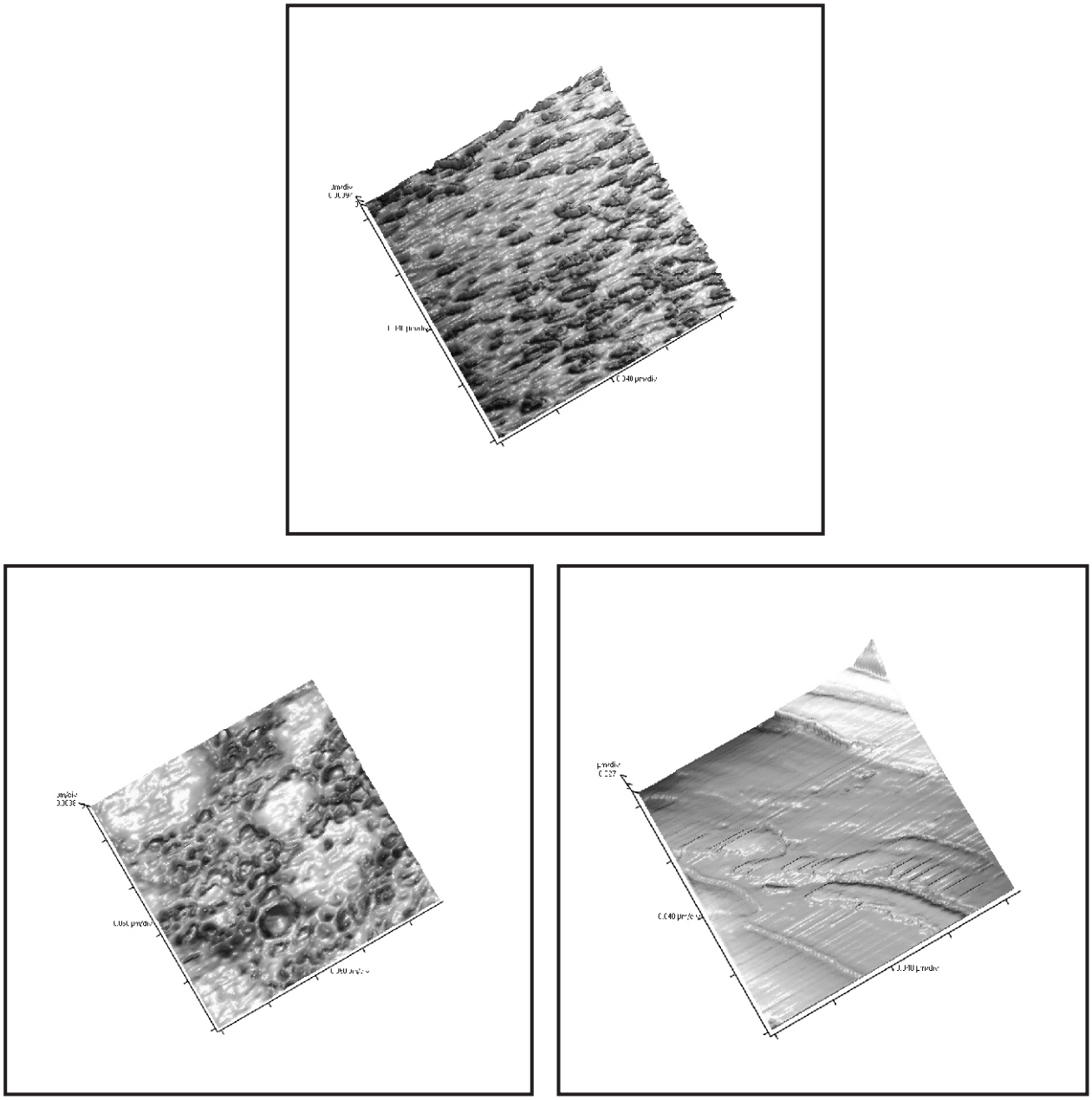

Figure 8: AFM images of (A) bare gold-coated glass (B) **4**-SAM and (c) **3**-SAM

CONCLUSION

Electrochemical impedance spectroscopy has been employed to probe the electrical integrity of self-assembled monolayers of some organosulphur-metal complexes, chemisorbed on polycrystalline gold disc electrode. Structural integrity of the SAMs was probed using atomic force microscopy. Impedance data, analyzed using suitable equivalent circuits, gave a qualitative estimate of electrical integrity of the SAMs. The nature of the metal and molecular features of the substituent, on the ligand skeleton, has direct impact on electrical integrity of the SAMs. The SAM-modified gold electrode (**3**-SAM), whose chemical modifier has an iron metal center and benzylthio substituent, has the most impressive impedance data. Values of charge transfer resistance, R_{CT}, double-layer capacitance, C_{dl}, and Warburg impedance, Z_W, recorded for the cell with **3**-SAM-modified gold electrode, are diagnostic of the fact that, the best electrically-conducting, of all the SAMs investigated, is **3**-SAM.The structural features of the SAMs were closely related to the molecular nature of the substituent, attached to the ligand framework of the modifier. The understanding offered by the results of this

work will be of immense benefit in the use of SAMs of these organosulphur-metal complexes for design of surfaces in electronic devices, corrosion prevention and the emerging field of supercapacitors.

REFERENCES

Akinbulu, I.A.; Khene, S. and Nyokong, T. 2010. Surface Properties of Self-Assembled Monolayer Films of Tetra-Substituted Cobalt, Iron and Manganese Alkylthio Phthalocyanine Complexes. *Electrochim. Acta*, 55, 7085-7093.

Akinbulu, I.A.; Ozoemena, K.I. and Nyokong T. 2011. Formation, Surface Characterization, and Electrocatalytic Application of Self-Assembled Monolayer Films of Tetra-substituted Manganese, Iron, and Cobalt Benzylthio Phthalocyanine Complexes. *J. Solid State Electrochem*, 15, 2239-2251

Allara, D. and Nuzzo, R.G. 1987. U.S. Patent #4, 690, 715.

Barsoukov J. and Macdonald R. 2005. Impedance Spectroscopy: Theory, Experiment, and Applications, second ed., John Wiley and Sons, Inc., Hoboken, New Jersey, (Chapter 1).

Boukamp, B.A. 1986. A Nonlinear Least Square Fit Procedure for Analysis of Immitance Data of Electrochemical Systems. *Solid State Ionics*, 20, 31-44

Brug, G.J.; van den Eeden, A.I.G.; Sluyters-Rehbach, M. and Sluyters, J.H. 1984. The Analysis of Electrode Impedances Complicated by the Presence of a Constant Phase Element. *J. Electroanal. Chem. and Interfacial Electrchem.*, 176, 275-295

Chen, J.; Reed, M.A.; Rawlett, A.M. and Tour, J.M. 1999. Large On-Off Ratios and Negative Differential Resistance in a Molecular Electronics Devices. *Science*, 286, 1550-1552.

Finklea H.O. 2000. In: R.A. Meyers (Ed.) Encyclopedia of Analytical Chemistry, Applications, Theory and Instrumentations, vol. 11, Wiley, Chichester, p. 10090-10115

Hsu, C.S. and Manfeld, F. 2001. Technical Note: Concerning the Conversion of the Constant Phase Element Parameter Y_0 into Capacitance. *Corrosion*, 57, 747-748.

Nuzzo, R.G. and Allara, D.L. 1983. Adsorption of bifunctional organic disulphides on gold surfaces. *J. Am. Chem. Soc.*, 105, 4481-4483

Nuzzo, R.G.; Zegarski, B.R. and Dubois, L.H. 1987. Fundamentals studies of the chemisorption of organosulphur compounds on gold (III): Implications for molecular self-assembly on gold surfaces. *J. Am. Chem. Soc.*, 109, 733-740.

Ozoemena, K.I.; Nyokong, T. and Westbroek, P. 2003. Self-Assembled Monolayers of Cobalt and Iron Phthalocyanine Complexes on Gold Electrodes: Comparative Surface Electrochemistry and Electrocatalytic Interaction with Thiols and Thiocyanate. *Electroanalysis*, 15, 1762-1770

Polymeropoulos, E.E. and Sagiv, J. 1978. Electrical conduction through adsorbed monolayers. *J. Chem. Phys.* 69, 1836-1847

Porter, M.D.; Bright T.B.; Allara D.L. and Chdsey C.E.D. 1987. Spontaneously organized molecular assemblies. 4. Structural characterization of n-alkylthiol monolayers on gold by optical ellipsometry, infrared spectroscopy, and electrochemistry. *J. Am. Chem. Soc.*, 109, 3559-3568

Sagiv, J. 1979. Organized monolayers by adsorption. III. Irreversible adsorption and Memory Effects in Skeletonized Silane Monolayers. *Isr. J. Chem.*, 18, 339-345

Sagiv, J. 1980. Organized monolayers by adsorption. 1. Formation and structure of oleophobic mixed monolayer on solid surfaces. *J. Am. Chem. Soc.*, 102, 92-98

Simpson, T.R.E.; Russell, D.A.; Chambrier, I.; Cook, M.J.; Horn, A.B. and Thorpe, S.C. 1995. Formation and Characterization of a Self-Assembled Phthalocyanine monolayer suitable for gas sensing, *Sens. Actuators B*, 29, 353-357